FLUID FORENSICS OF FOSSILS

A DEEP-SEA VELOCIMETRY JOURNEY INTO HOW ANCIENT CREATURES FED

CALLUM COGHLAN, PROFESSOR BEN WILLIAMS & PROFESSOR ALFONSO CASTREJON-PITA

ABSTRACT

In palaeontology, life from the Ediacaran period (641–535 million years ago) remains poorly understood. There is currently a lack of evidence on how different species anchored themselves to the sea floor and took in nutrients. A growing body of research using either computer simulations or mechanical experiments to analyse water flow around these species has provided some answers, but a lack of cross-validation between experimental and computational work limits the power of their conclusions. This project aimed to be the first to combine particle image velocimetry (PIV) and particle tracking velocimetry (PTV) flow-field visualisation experiments with computational fluid dynamics (CFD) simulations to ascertain how the *Charnia masoni* (Fig. 1), thought to be one of the first instances of animal life from this period, lived and fed. A rig was devised for flow visualisation experiments on 3-D printed models of the *Charnia* (Figs. 2 & 3), including a novel magnet-based technique for moving the models around the flow section without any disassembly. Whilst the Covid-19 pandemic prevented most experiments from taking place, conclusions about how *Charnia* may have anchored itself are presented here based on the drag force experienced by the models. Further, the pandemic provided an opportunity to develop a novel MATLAB tool for PTV analysis of double-frame images to be developed so future studies can be undertaken exclusively with PTV. This removes the need for expensive PIV equipment and ultimately enables swifter collection of knowledge on these enigmatic creatures.

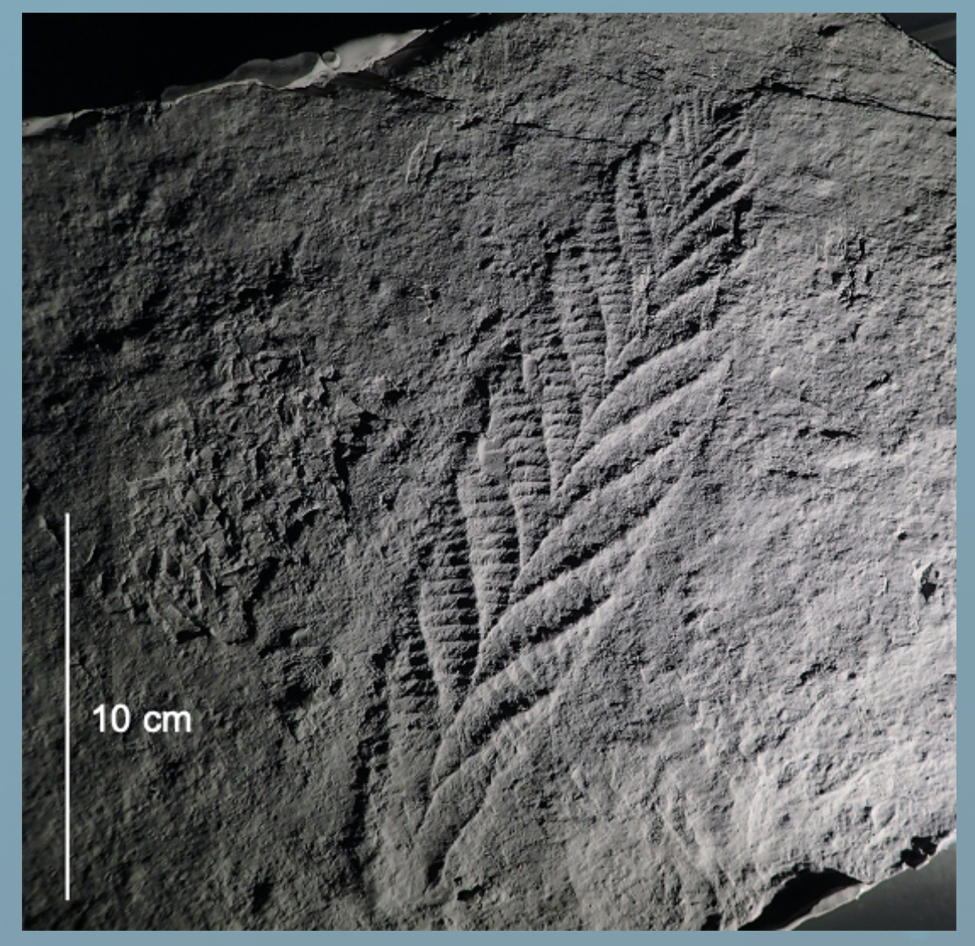

Figure 1: *Charnia* fossil discovered in 1958[1]

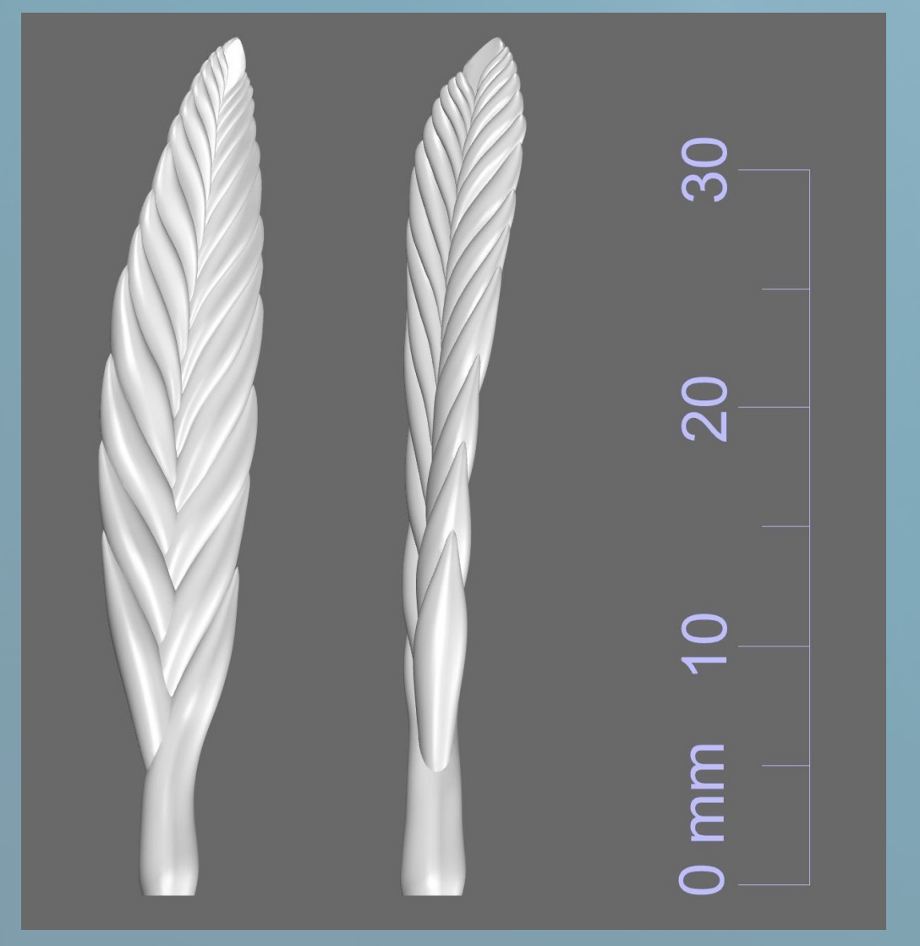

Figure 2: Solidworks model of the fossil[2]

Figure 3: 3-D printed model for this project

METHODS

Feeding Mechanisms

Previous study suggests two widespread feeding mechanisms for Ediacaran species:

1. Osmotrophy, by which dissolved organic nutrients are taken up osmotically. Osmosis is a passive process, so its efficiency is reliant on flow being spread evenly across the entire surface area of the osmotrophic organism.
2. Suspension feeding, by which particles of food are sifted from the water. Suspension feeders rely on water being passed through specialised structures which trap nutrient particles. The flow-field around such organisms should therefore be more specific, with flow being directed to these structures.

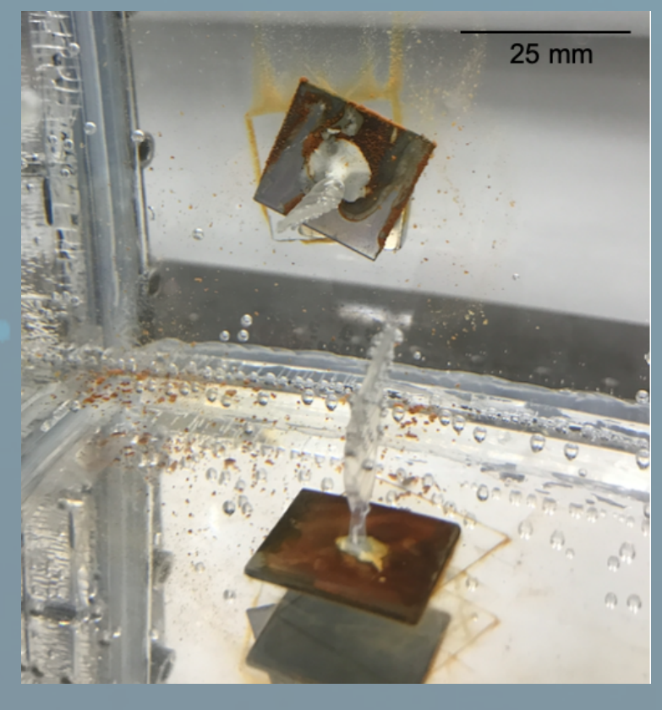

Figure 5: Models mounted on magnets

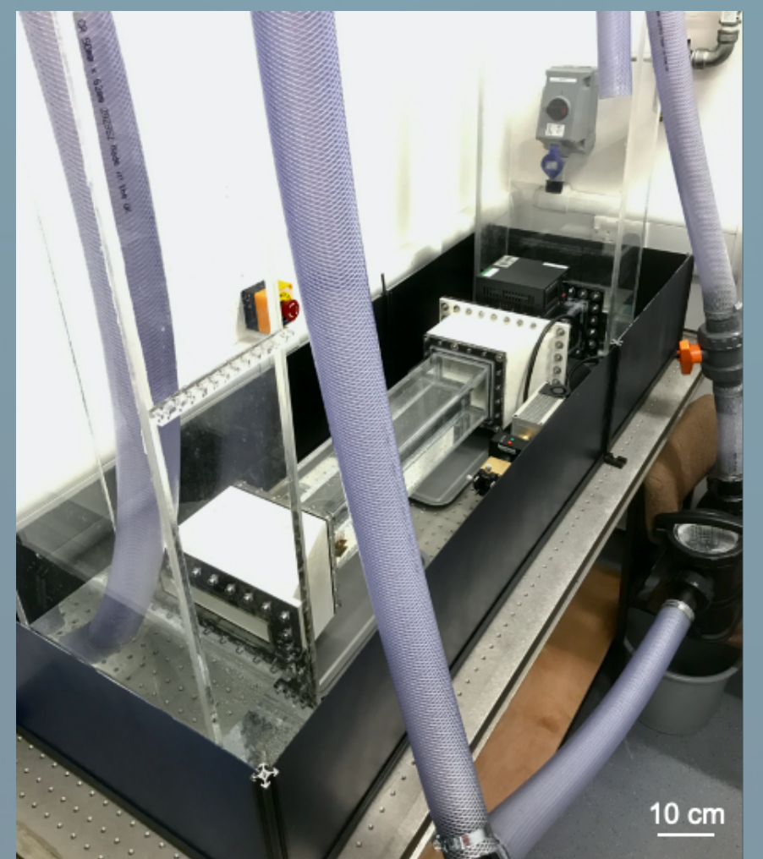

Figure 4: Photo of the experimental rig

A Rig to Simulate the Flow (Figs. 4 & 6)

- Flow straightener: ensures flow is laminar
- Nozzles: redirect the flow into the acrylic central flow section, where the *Charnia* fossil model, 3-D printed from a flexible resin, is held in place;
- EPDM/latex rubber seals: water-tightness;
- Pipes: connect the pre-filled tanks to a swimming pool pump, which circulates water right-to-left past the model.
- Valve: fitted in the pipework to control the flow rate.
- Designed for flow speeds of up to 0.45 m/s – accounts for typical deep ocean currents of up to 0.4m/s
- Models glued to thin steel sheets. held in place via magnets placed on the outer face. These could be moved by hand to move the models around the test section without having to dismantle any of the set-up, an innovation intended to make testing more rapid later in the project (Fig. 5).

The majority of the equipment was designed from scratch specifically for this project, with nothing set up in advance in the laboratory space.

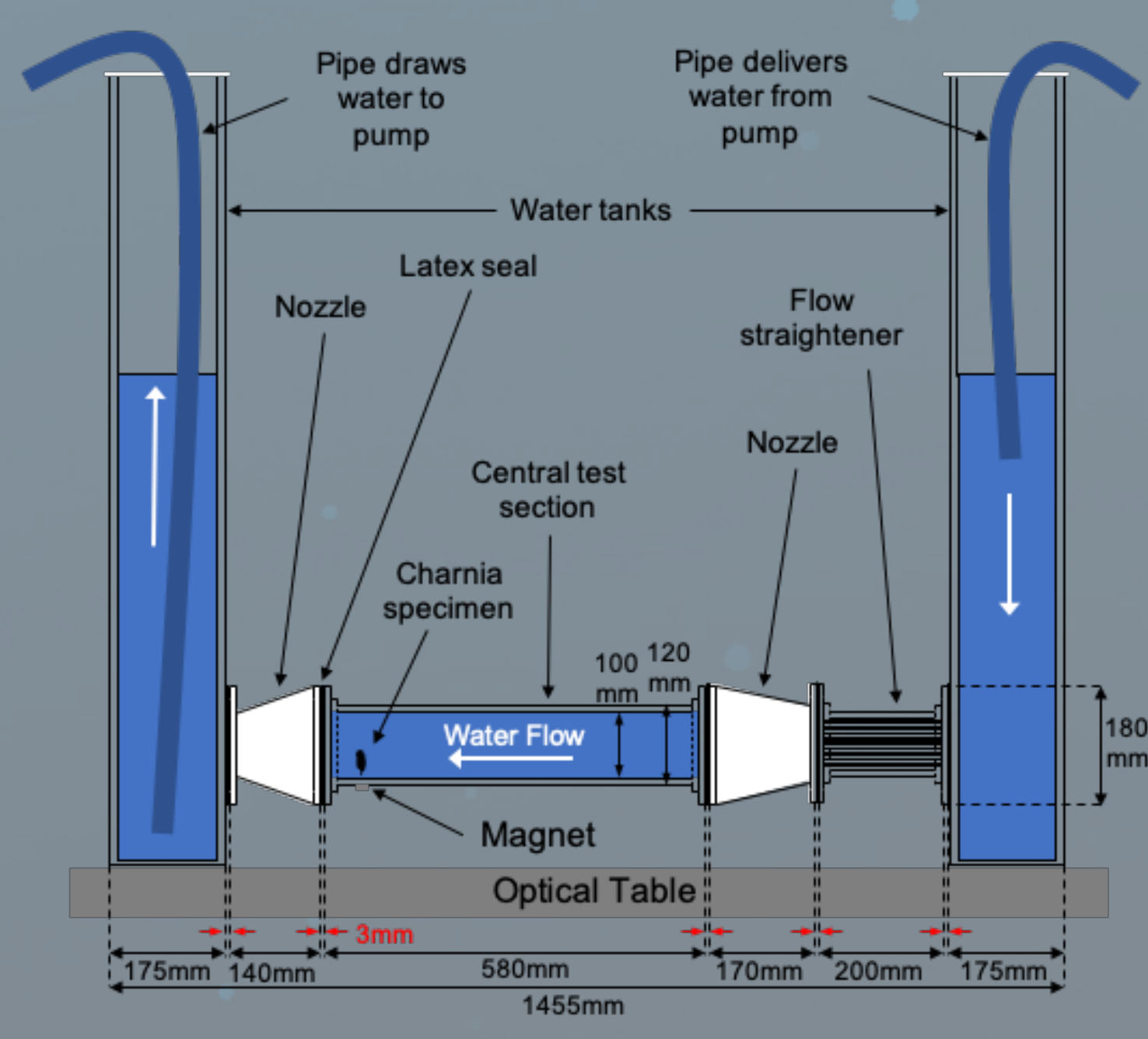

Figure 6: Schematic of the experimental rig

An Optical Set-up to Image the Flow

Imaging would have been done using PTV and PIV, before Covid-19 shut down the lab

1. For PTV: a compact diode-pumped solid-state laser delivered a continuous laser sheet in a plane through the transparent central flow section.
2. For PIV: a pulsed laser would have been used instead.

Fig. 7 illustrates the optical system. The camera was mounted above the test section such that the lens pointed down at the model. This allowed for two different model planes to be imaged, fully interrogating the flow without having to adjust the laser input direction. This is better for laser safety.

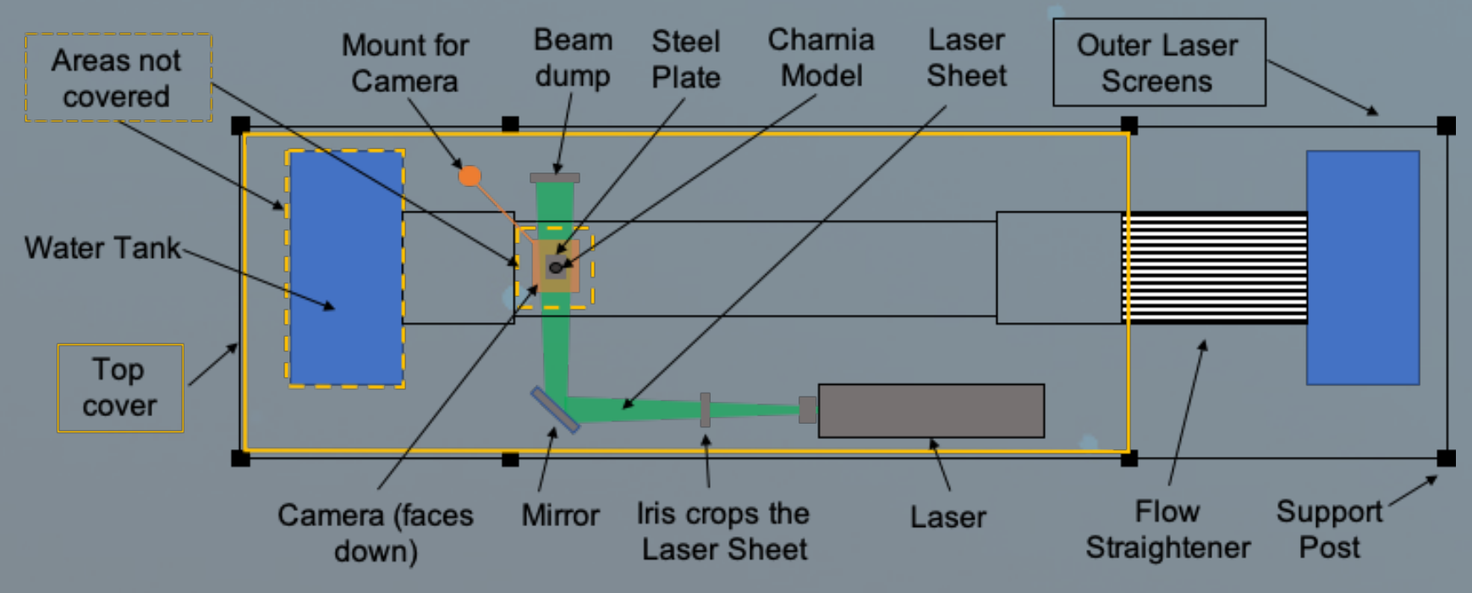

Figure 7: Optical set-up diagram

MEASURING THE FLOW

PTV vs PIV

Both are instantaneous flow measurement techniques that measures flow velocity and direction in a particular field of view via tracer particles whose size and density are carefully chosen to follow the flow dynamics as closely as possible. Two images are taken micro/nanoseconds apart with a double-frame camera and the tracer particles, illuminated by a laser sheet, are tracked between the frames to provide the velocity profile using a coded analysis tool.

Particle Image Velocimetry (PIV):

- Eulerian – the movement of all particles in the frame is analysed at once.
- Windows of analysis – each frame is broken down into smaller windows containing enough particles to find the localised velocity field in the window.
- Pulsed laser – pulses need to be calibrated with the double-frame camera exposures so that the particles are illuminated at the right times
- Was intended to be used in this project for the majority of the experiments, with velocity-field analysis undertaken using PIVLab[4]. A typical output is shown in Fig. 8 – the arrows are sized according to their associated velocity magnitude.

Particle Tracking Velocimetry (PTV):

- Lagrangian – each tracer particle is individually tracked between frames.
- No smaller windows required, and a continuous laser suffices.
- Would have been used here to qualitatively confirm that the flow through the test section was as designed for.

When Covid-19 struck, we were just about to start taking images of the flow around the *Charnia* model. Instead the lab shut down and the project switched focus to creating a bespoke tool for PTV analysis with similar functionality to PIVLab. Whilst some similar tools for PTV exist, this is one of the first to use the fact that the second exposure of the double-frame camera is longer than the first to figure out the direction of the flow (Fig. 9).

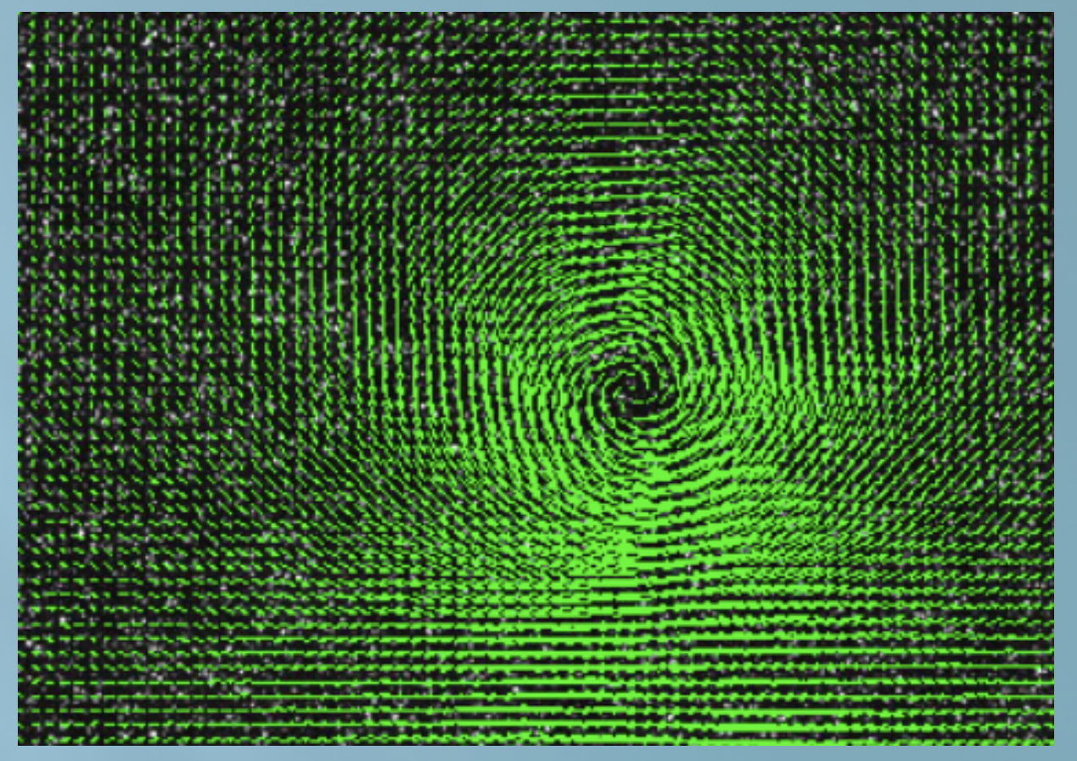

Figure 8: PIV analysis output velocity field

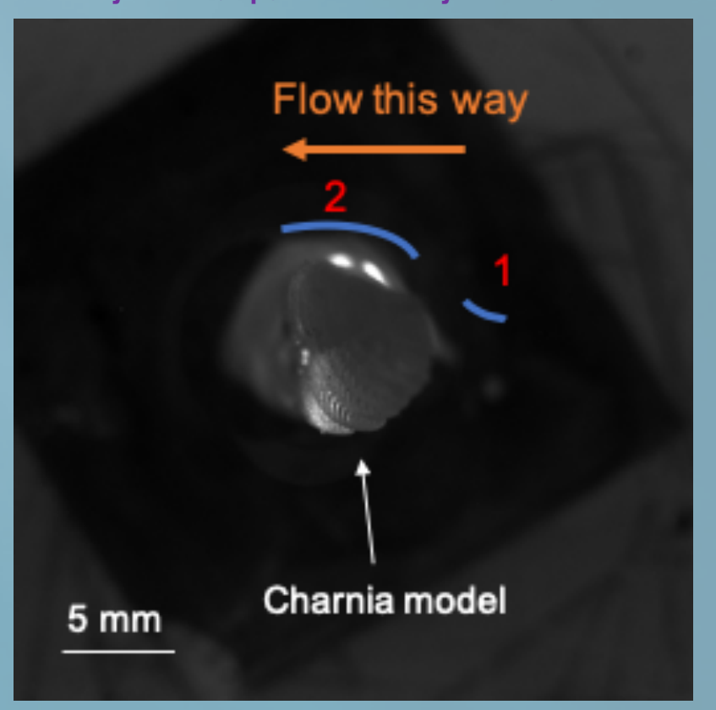

Figure 9: What double-frame images may have looked like round the *Charnia*

PTV Algorithm Objectives

The tool was designed to:

1. Load in a pair of double-frame camera images of flow around the *Charnia* model;
2. Identify the seeding particles in each frame – they appear as streaks. The streak in frame two is longer due to longer exposure to the laser sheet. Use thresholds to ignore noise and large objects such as the model itself;
3. Extrapolate the predicted path for each longer second frame streak using various poly-fits;
4. Find the closest first frame streak for each poly-fit, and choose the closest of these – this first streak is usually the correct match for the second;
5. Use the appropriate poly-fit to plot each trajectory from the start of the first streak to the end of the second;
6. Split each trajectory into three velocity vectors and calculate these velocities based on calibration provided by the user;
7. Allow the user to remove anomalous velocity vectors by selecting them on the plot

The final output is a plot of velocity vectors and a matrix containing their velocities. For simulated images, each overall trajectory also has a coefficient representing how well the original trajectory has been returned – this is the goodness of fit coefficient C_{GOF}. The figures below demonstrate various stages of development of the tool for simulated images of potential flow around a cylinder – approximating flow around the *Charnia* model looking top-down.

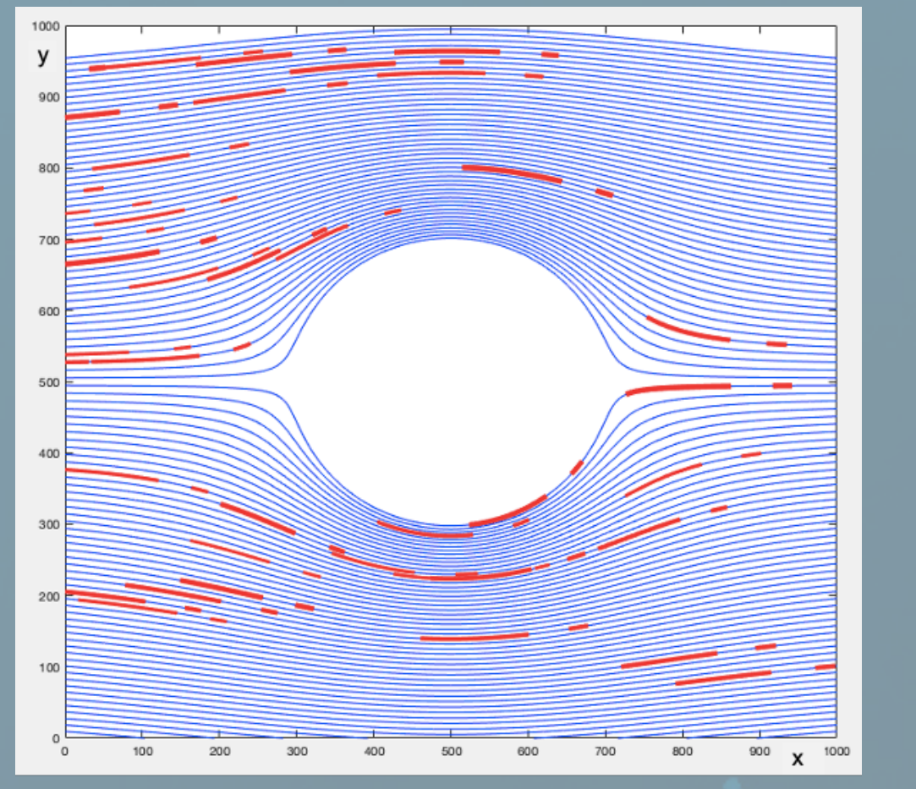

Figure 10: Simulation of potential flow. Red lines are the seeding particle streaks for analysis

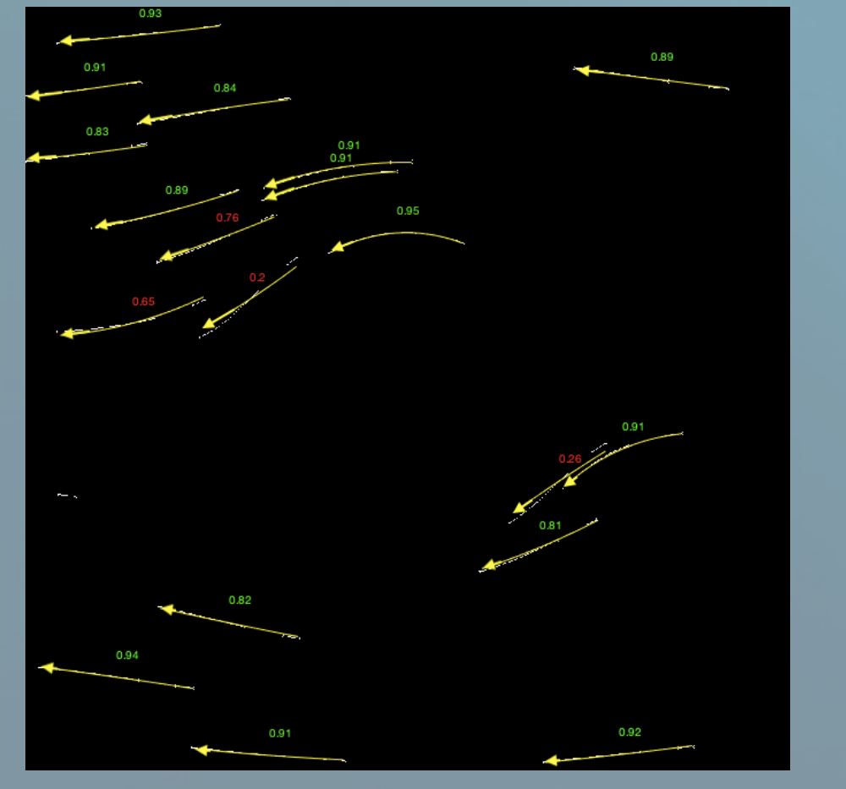

Figure 11: A set of trajectories returned by the tool using only arc fits. Wide spread of C_{GOF}.

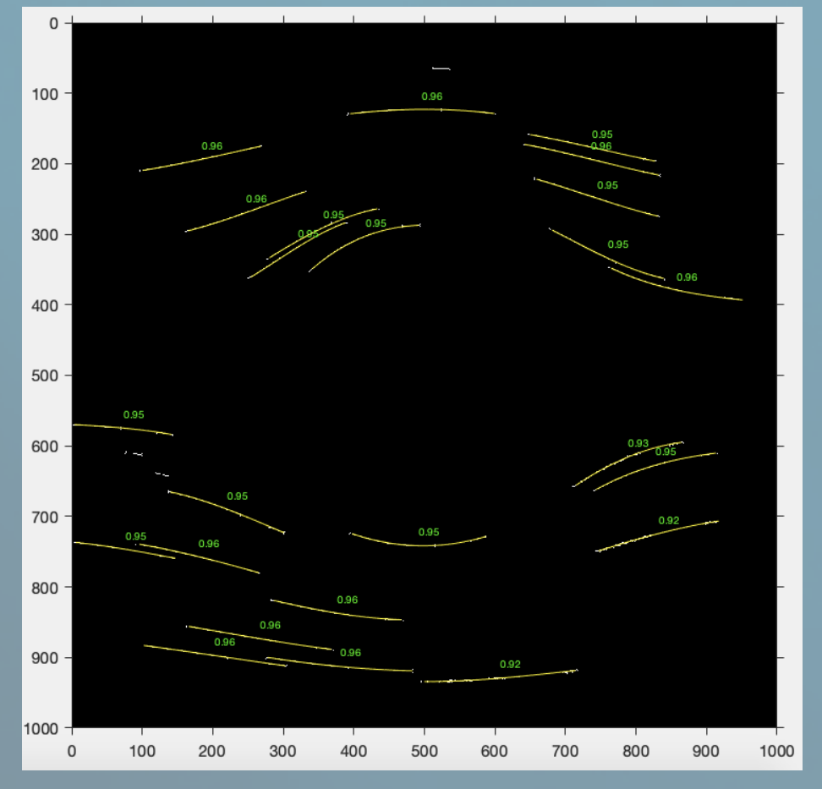

Figure 12: Huge improvement in C_{GOF} when 3rd-order poly-fit has been added to the tool

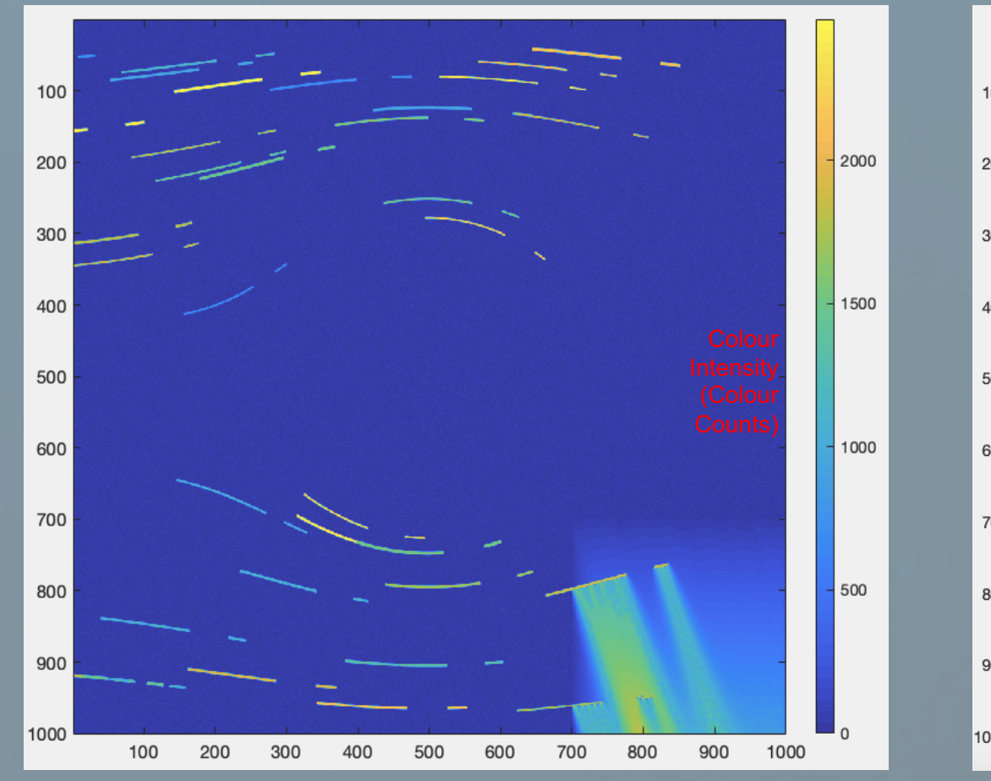

Figure 13: Simulating a pair of double-frame images of potential flow, with a noisy region bottom right

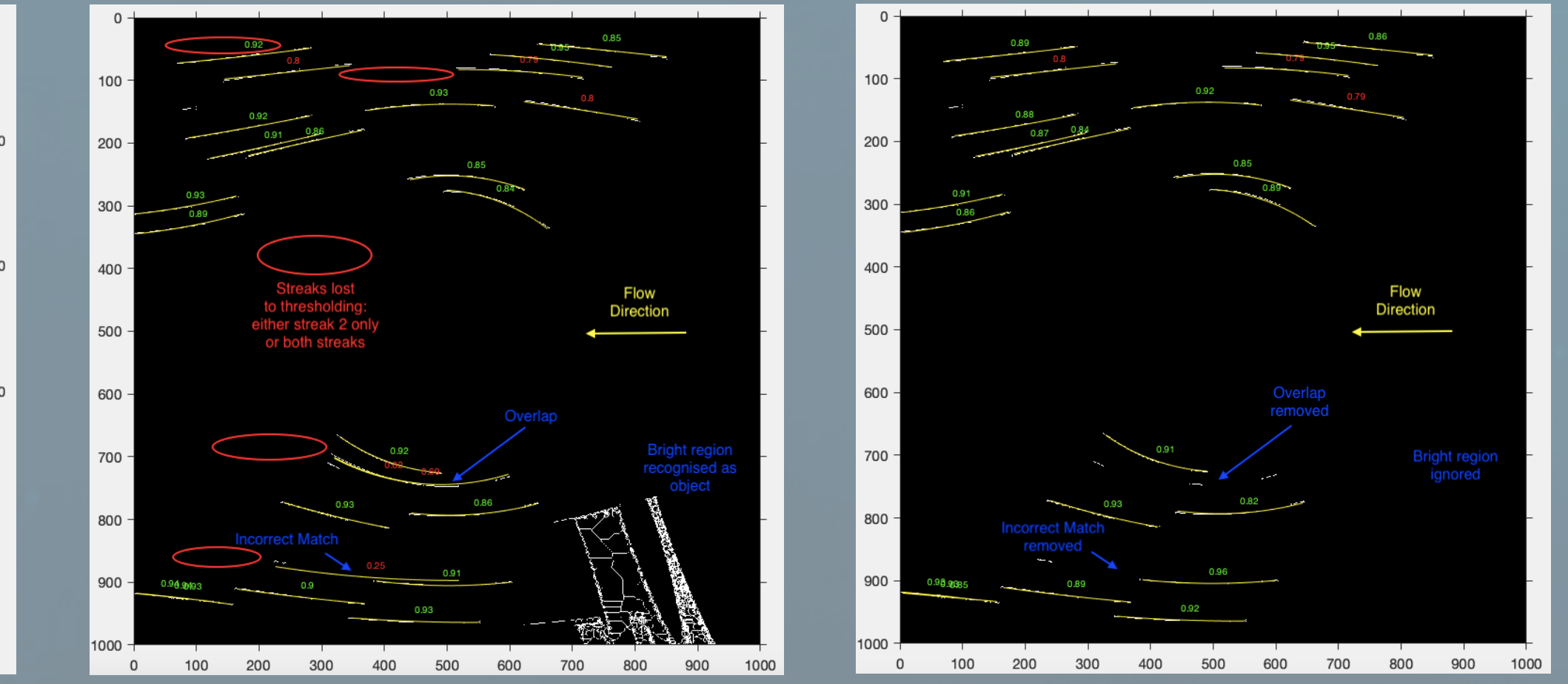

Figure 14 & 15: Tuning the intensity and object size thresholds for object recognition such that the noisy region and overlapping trajectories are ignored

Algorithm Performance

After only eight weeks of development, this PTV analysis tool offers most of the same functionality as PIVLab. Both tools provide:

- Arrow-based visualisations of the velocity flow-fields;
- Quantitative velocity data;
- The ability to remove anomalous vectors.

PIVLab also provides users with further post-processing options, for example colour-grading the vectors based on their absolute velocity values. The newly-developed PTV tool is also more tailored to the double-frame camera which would have been used for this project's experiments. The tool has a high successful match rate and C_{GOF} is very high thanks to a range of poly-fits being trialled for each streak pair. Going forwards, the velocity flow-field around the *Charnia* could be analysed exclusively with PTV – advantageous because it is both cheaper and easier to set up than PIV.

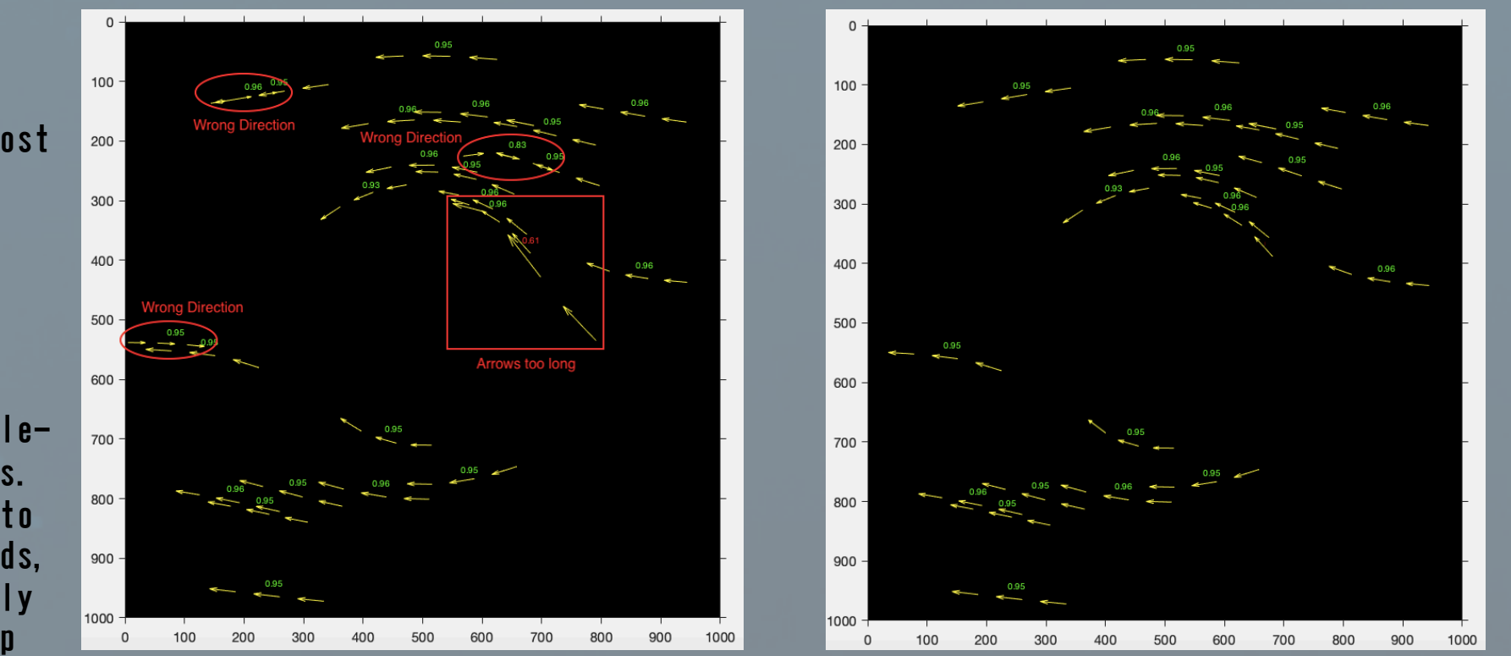

Figure 16 & 17: Anomalous vectors can be removed simply by clicking them on the plot

ANALYSING THE FLOW

All flow analysis was based on photos and videos of the apparatus hastily taken before lockdown started. The accuracy may be compromised as a result. Nevertheless, the analysis does allow for some conclusions to be drawn about the anchorage of the *Charnia*

Flow Speed from Smartphone Footage

PTV would ideally have been used to calculate the water velocity through the central flow section. Instead, smartphone videos of the flow with the pump valve fully open were analysed to verify whether the maximum flow velocity was the 0.45 m/s predicted. Air bubbles not yet flushed out of the flow were tracked across the video frame (Fig. 18). Each streak was tracked for a certain number of frames, from which a speed was ascertained. Tracking ten streaks across two camera angles yielded an average flow speed of 0.54 m/s. The main contributor to this overestimate was speculating the position of the streak relative to the model in order to estimate its physical length.

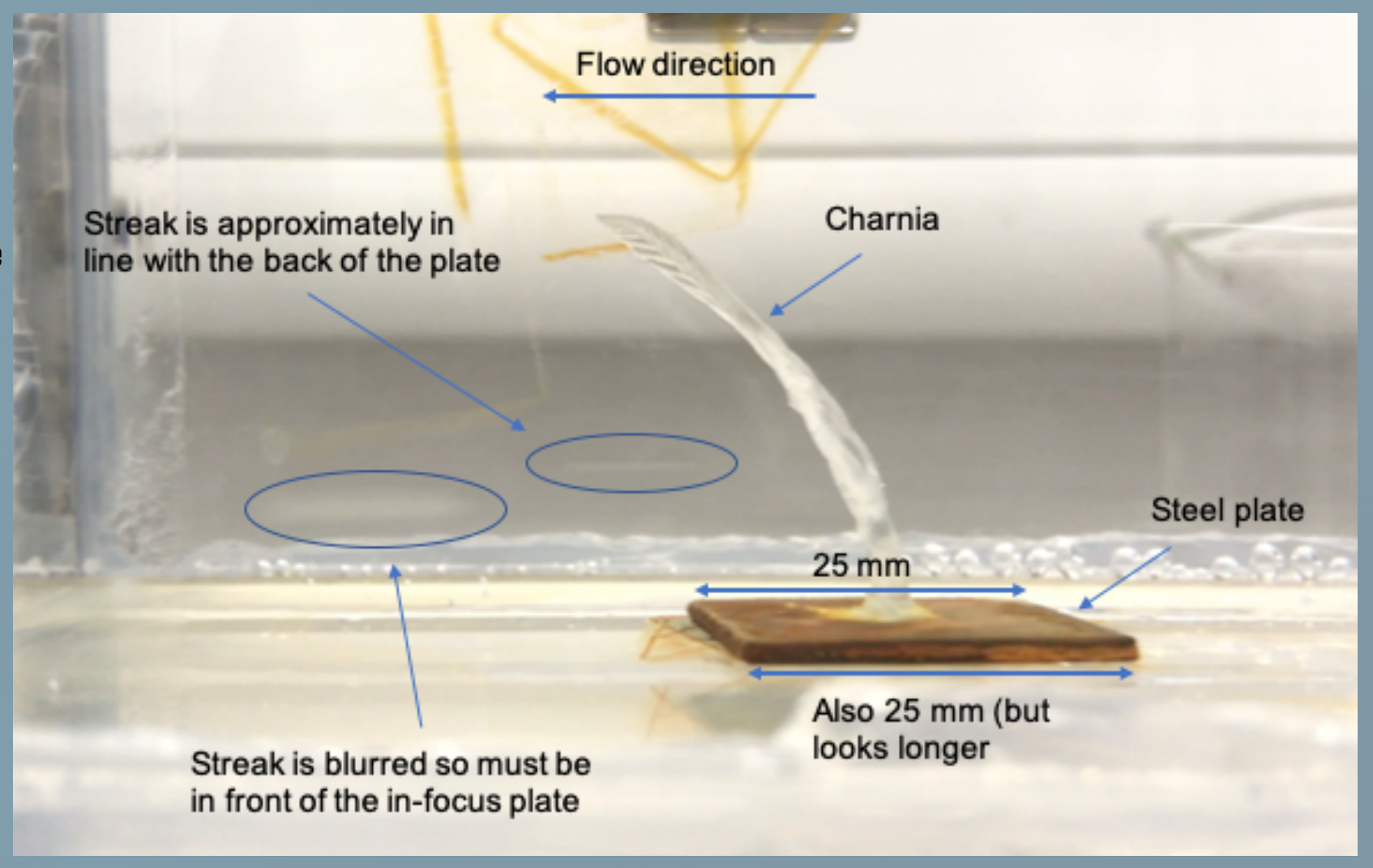

Figure 18: One camera angle for air bubble velocity calculations

Drag Force from Deflection Analysis

At this high flow speed, the *Charnia* model experienced a substantial deflection of approximately 20 mm. By modelling the specimen as a cantilever beam, moment and beam bending analysis provided an estimate of the drag force acting on it. The wider face of the model, facing into the flow, was approximated as a diamond, providing the drag loading profile in Fig. 19. The relationship between the peak central load and the 20mm deflection at the tip was found as follows:

- The overall profile was split into two separate loading profiles (Fig. 20);
- Taking a cut at position x, the moment M at x was calculated (Fig. 21);
- Subsequent integration and beam bending analysis yielded a value for peak drag on the model as $d_{0,\,upper} = 0.079$N;
- The diamond shape is an underestimate for the area of the model. For a rectangular shape, an overestimate, the uniform loading gives $d_{0,\,lower} = 0.049$ N.

An estimate for the drag calculated via the drag coefficient and the predicted loading on the magnets was 0.046 N, on the same order and only just outside the above range, corroborating this beam deflection analysis.

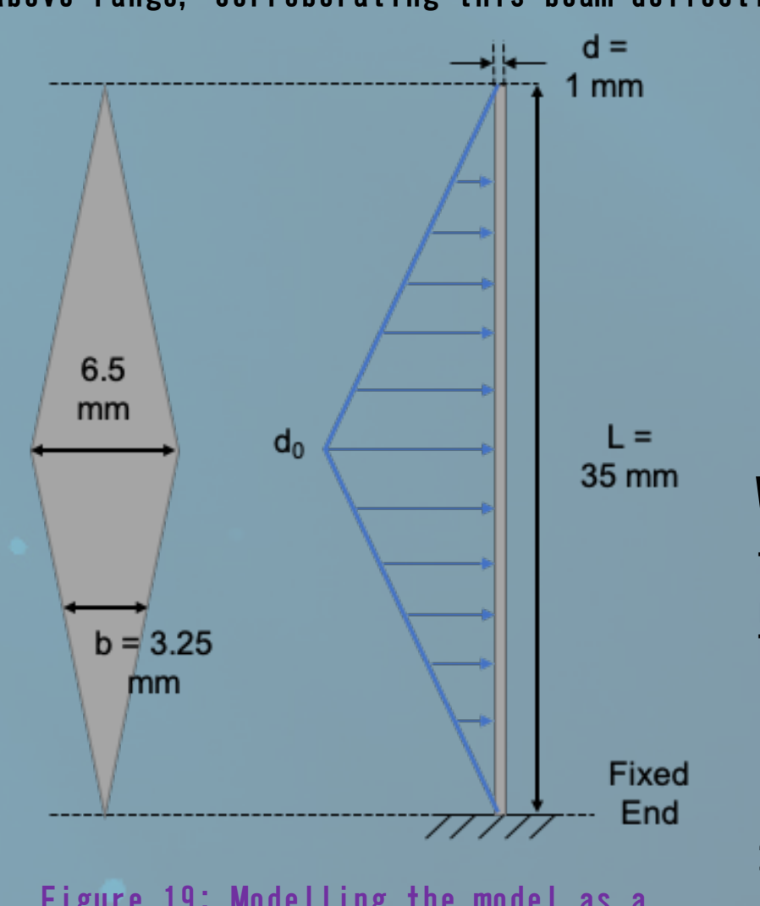

Figure 19: Modelling the model as a cantilever with diamond front area and loading profile

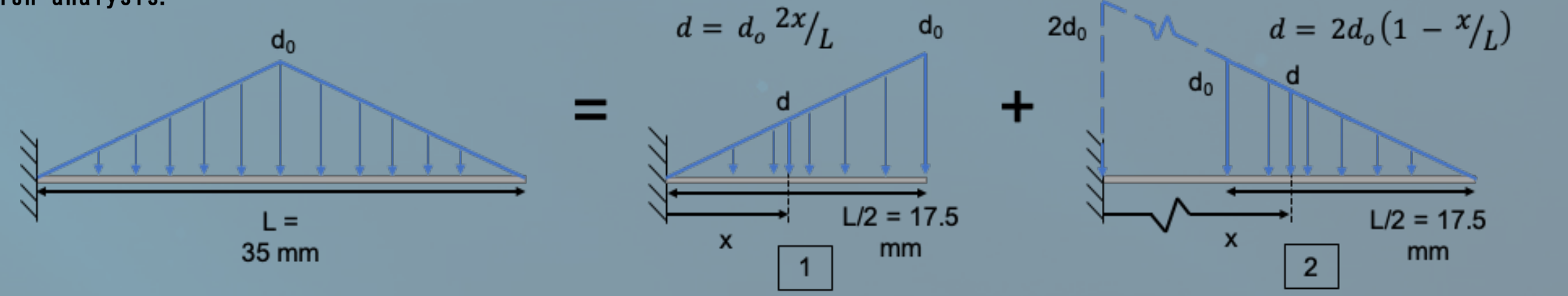

Figure 20: Splitting the overall profile into two loading profiles

What Does this Tell us about the *Charnia*?

The estimates for flow speed and drag force are remarkably close to those predicted by the theory.
The drag value provides insight into its behaviour:

1. The deflection was over half the height of the model (35 mm). For the *Charnia* to not be swept away by fast ocean currents, it must have been strongly anchored to the ocean floor.
2. It must have had similar properties to the elastic resin used for the models in order to be flexible enough to withstand the drag.

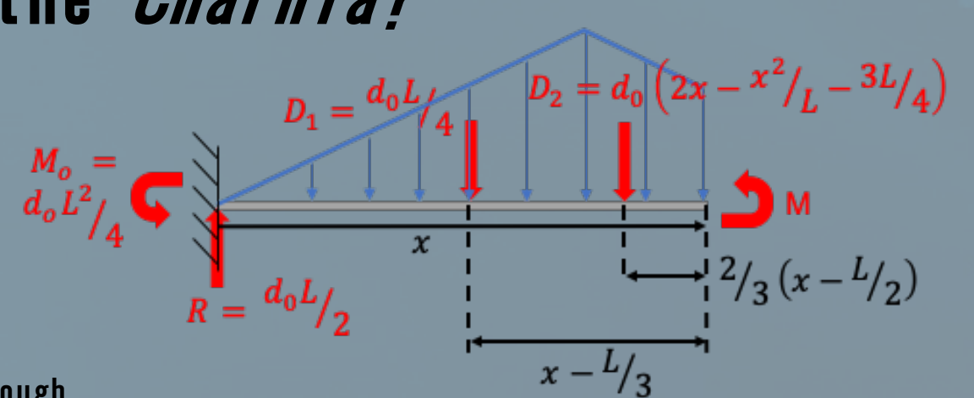

Figure 21: Moment Analysis along the model

The model would have experienced a smaller drag and lower deflection had the narrower side been facing into the flow. This would evidently be the ideal orientation, but the twist in the models means that such an orientation would be very tricky to achieve in practice. The twist could even result in the wide side always being turned to face into the flow. Further experiments to determine whether the orientation of the model remains fixed depending on its initial exposure direction would provide more insight into this theory, or whether the species was capable of facultative mobility.

CONCLUSIONS

The initial objectives were met as follows:

- The experimental rig was designed, constructed and assembled from scratch, with water successfully circulating around the system;
- The novel magnet mounts enable new experimental variations to be devised without any disassembly;
- The small amount of data that could be gathered indicated that *Charnia* would have experienced substantial drag with its wider side facing into the flow, suggesting that facultative mobility may have helped reduce the forces they felt.

The revised objectives when Covid-19 forced us to pivot the focus of the project were met as follows:

- An algorithm was devised to undertake particle tracking velocity (PTV) analysis by matching particles between two image frames taken in quick succession and returning their velocities;
- The matching algorithm was improved via testing with more complicated simulations including arced flow and potential flow around a cylinder – the algorithm returns a coefficient for how closely the returned vectors follow the simulated trajectories (C_{GOF});
- Post-processing tools allow the user to remove anomalous velocity vectors from the output figure;
- The entire algorithm can be run multiple times for the same scenario, allowing for a more complete picture of the flow to be ascertained by overlaying all the velocity vectors (An example in Fig. 22).

The novel PTV tool successfully provides the same necessary functionality as other more general existing tools for particle image velocimetry (PIV) such as PIVLab, such that PIV will be unnecessary for this particular fossil flow-field analysis going forwards.

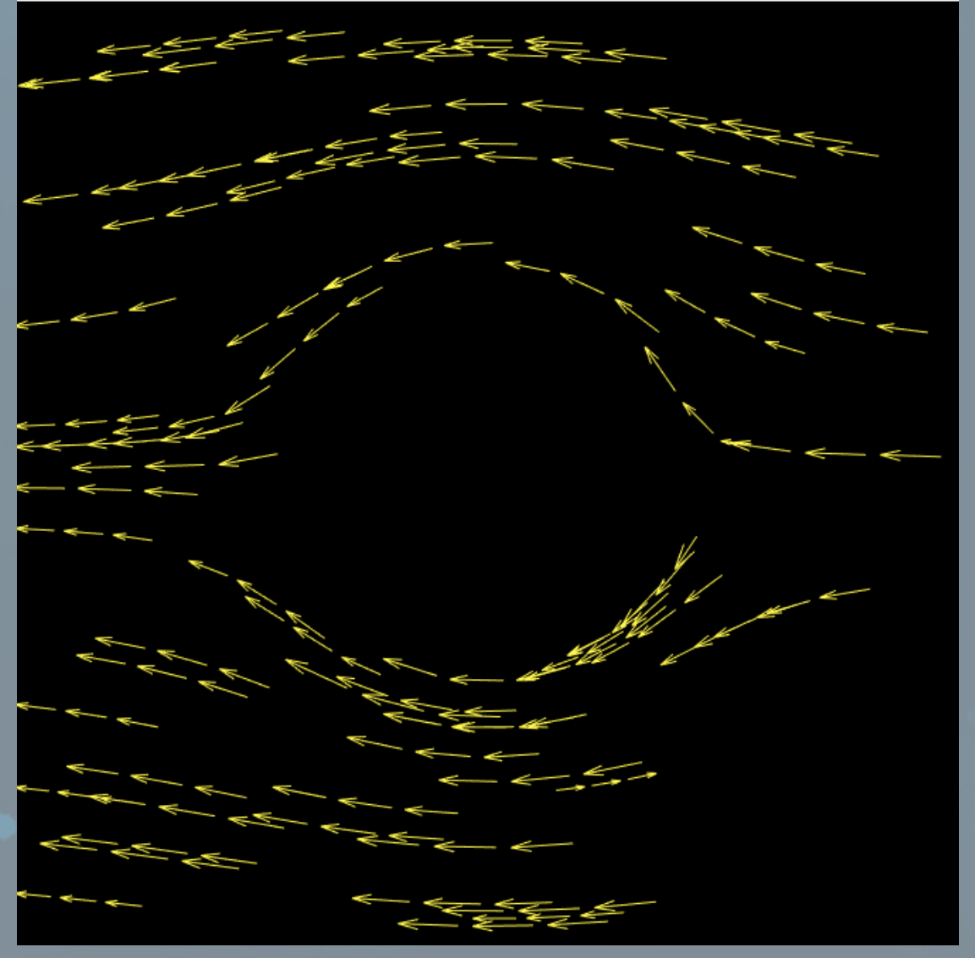

Figure 22: Velocity field for four post-processed simulations of potential flow

Further Work

The entire set-up including the optical equipment and protective guards can easily be reassembled in a few hours, enabling future PTV experiments to take place on the *Charnia* models: lockdown was the only factor preventing the experimental objectives from being met. Further experimentation will be needed to gather PTV velocity data around the models. This data could then be used to choose between osmotrophy and suspension feeding as the likely feeding model, alongside comparison with CFD modelling already undertaken (Fig. 23).
Further improvements to the algorithm include building in more poly-fits to improve C_{GOF} for randomly shaped velocity vectors and testing the algorithm with more real-life PTV image pairs.

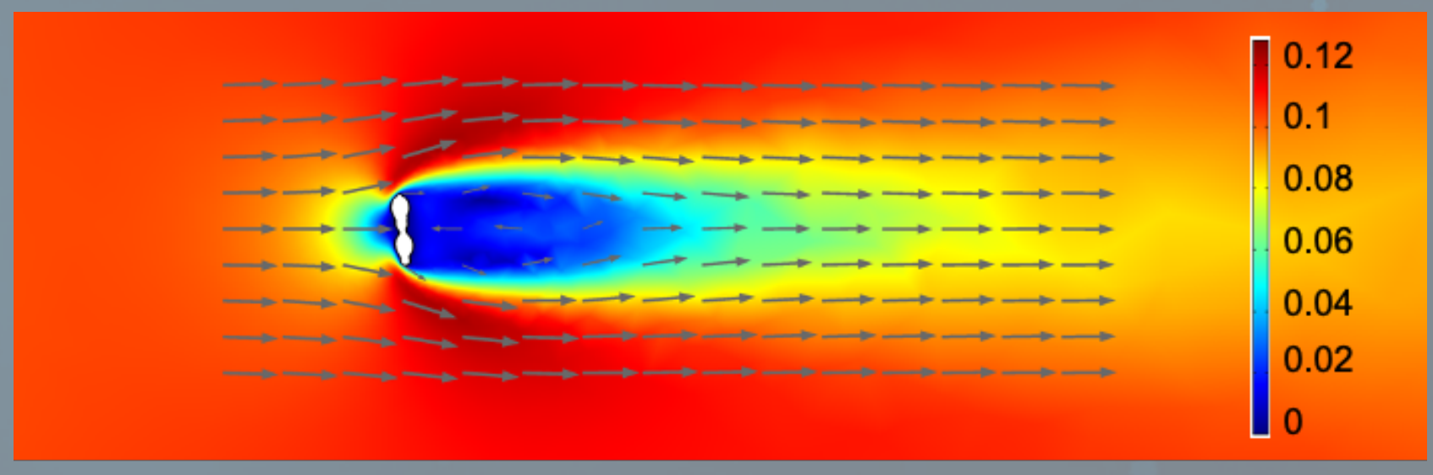

Figure 23: Top-down CFD model of flow around a *Charnia* [4]

In conjunction with
Dr Imran Rahman
at the
Oxford University Museum of
Natural History

Department of Engineering Science
University of Oxford

callum.coghlan@btinternet.com
https://www.linkedin.com/in/callum-coghlan-aabb68194/

REFERENCES

[1] T. Ford, "Precambrian fossils from charnwood forest," *Yorkshire Geological Society Proceedings*, vol. 31, no. 3, pp. 211-217, 1958.
[2] "Mighty Fossils," http://mightyfossils.com, 2019
[3] W. Thielicke, "PIVlab - particle image velocimetry (PIV) tool," https://uk.mathworks.com/ matlabcentral/fileexchange/27659-pivlab-particle-image-velocimetry-piv-tool, 2019
[4] Kindly provided by Dr Imran Rahman, Deputy Head of Research at the Oxford Museum of Natural History